JBAT 13(1) (2024) 38 – 47

Jurnal Bahan Alam Terbarukan

Accredited SINTA 2 by Ministry of Research and Technology/National Research and Innovation Agency
SK No. 200/M/KPT/2020
http://journal.unnes.ac.id/nju/index.php/jbat

p-ISSN 2303 0623
e-ISSN 2407 2370

Surface Evaluation of Tricalcium Phosphate Bioceramic Coating on SS-316L by Electrophoretic Deposition

Gita Novian Hermana[1, ✉], Dhion Khairul Nugraha[2], Muhammad Rizki Gorbyandi Nadi[3], Moch. Wisnu Arif Sektiono[4], Randy Mediawan Mayello[3], Miftah Farhan[3], Nirmala Cahya Kusuma[3], Naufal Alden Alfayed[3], Fauzi Muhamad Rizqi[3]

DOI: https://doi.org/10.15294/jbat.v13i1.49639

[1] Department of Advanced Materials Engineering, Politeknik Manufaktur Bandung, Bandung 40135, West Java, Indonesia
[2] Department of Manufacture Engineering, Politeknik Manufaktur Bandung, Bandung 40135, West Java, Indonesia
[3] Department of Advanced Materials Engineering, Politeknik Manufaktur Bandung, Bandung 40135, West Java, Indonesia
[4] Department of Mechanical Engineering, Politeknik Negeri Malang PSDKU Kota Kediri, Kediri, 64114, Indonesia.

Article Info

Article history:
Received
6 Januari 2024
Revised
14 April 2024
Accepted
30 May 2024
Online
June 2024

Keywords:
Tricalcium phosphate; Coating; Electrodeposition; SS316L; microstructure

Abstract

The development of orthopedic implant materials has become an important topic of discussion lately. The SS-316L alloy is widely used as an implant material due to its relatively low cost, corrosion resistance, and ease of production. However, metal alloys, especially SS-316L, are prone to ion release into the blood over time. Therefore, TCP or tricalcium phosphate [$Ca_3(PO_4)_2$] is needed to coat the surface of SS-316L, preventing ion release into the blood and enhancing the biocompatibility of the implant material. In this study, TCP coating was applied to the SS-316L substrate using the electrophoretic deposition technique. The influence of deposition time on changes in microstructure and mechanical properties is the main focus of this study. The results of the coating technique indicate that the deposition yield increases with the deposition time. Morphological testing results show that increasing deposition time improves coating quality by increasing the thickness of the coating layer and preventing layer peeling. The coating process also reveals the accumulation of layers in certain areas and the formation of thin layers in other regions. A deposition time of 30 minutes results in a coating thickness ranging from 48.7 to 57.9 µm. Hardness testing, conducted with indentation loads of 50, 100, and 300 gf, indicates that longer deposition times and higher indentation loads during hardness testing result in reduced material hardness.

INTRODUCTION

The global demand for healthcare devices, especially bone tissue implants, is increasing each year due to the growing aging population and other health factors (Drevet & Benhayoune, 2022; Gheno et al., 2012; Li et al., 2017). Therefore, current developments in orthopedic or dental surgeries are limited to inert metals such as titanium alloys, stainless steel, and CoCr alloys (AlMangour et al., 2020; Drevet et al., 2018; Farrakhov et al., 2021; Koumya et al., 2021; Nkonta et al., 2021; Sheremetyev et al. 2022; Trincă et al., 2021). This alloy is used because it has mechanical properties suitable for bone tissue replacement and has good biocompatibility with the body environment. According to the International Union of Pure and Applied Chemistry (IUPAC), biocompatibility is

✉ Corresponding author:
E-mail: gitanovianh@polman-bandung.ac.id

the ability of a material to come into contact with biological systems without causing deleterious effects (Drevet & Benhayoune, 2022; Ghasemi-Mobarakeh et al., 2019).

Stainless steel 316 L (SS-316L) has earned a wide reputation as an implant in reconstructive surgery due to its excellent mechanical, biomedical and chemical properties. Coated SS-316L is of particular interest in metal implants to stabilize biological structures (e.g. building bone tissue and creating joint prostheses) and accelerate the healing process or replace damaged biological tissue (Koumya et al., 2021; Kurgan, 2013) However, the main problem of SS-136L metal is related to its low bioactivity and biocompatibility. To avoid this problem, coating SS-136L metal with biocompatible and bioactive materials using tricalcium phosphate was proposed (Hosseinalipour et al., 2010).

The material used for surface modification of SS-316L is a biomaterial based on tricalcium phosphate (TCP, [$Ca_3(PO_4)_2$]), which exhibits excellent biocompatibility when used inside the human body (Anselme, 2000; Dorozhkin, 2015; Fiume et al., 2021). Additionally, TCP biomaterials possess osteoconductivity, non-immunogenicity, and the ability to stimulate strong bonding with bone tissue. TCP coating on SS-316L as a surface modification aims to overcome the poor mechanical properties of bioceramics. Therefore, TCP/ SS-316L composite material is proposed to overcome the problems of less active bioactivity of SS-316L and poor TCP mechanical properties (Tulinski & Jurczyk, 2012). The bioactive TCP coating over SS-316L, which is similar to the main mineral component of human bone, not only acts as a barrier layer but also promotes the natural growth of bone cells (Ma et al., 2022; Shao et al., 2016; Yuan et al., 2023).

There are different methods to create a calcium phosphate coating on the implant surface, such as plasma spraying (Chambard et al., 2019; Heimann, 2016), magnetron sputtering (Safavi et al., 2021; Surmenev et al., 2021; Surmeneva et al., 2019), pulsed laser deposition (Popescu-Pelin et al., 2017), deposition electrophoresis (Bartmanski et al., 2017; Kollath et al., 2013) or electrodeposition (Olivier et al., 2020a; Olivier et al., 2020b; Vidal et al., 2019). Electrophoretic deposition and electrodeposition are alternative methods to synthesize calcium phosphate films at low temperatures (Gao et al., 2018; Shirkhanzadeh, 1998). Electrophoretic deposition (EPD)-based coating processes have been carried out, including ceramic thick film deposition, lamination and body forming (Boccaccini et al., 2010; Caicedo et al., 2020). Electrophoretic deposition for TCP biomaterials on stainless steel metal is the most practical technique because it is inexpensive and relatively simple technique. This allows a more homogeneous TCP biomaterial layer to be achieved on the surface (Ananth et al., 2015). The deposition rate can be controlled by changing certain parameters such as electrode voltage and deposition time (Bai et al., 2010).

This study focuses on observing the microstructural evolution of a TCP biomaterial deposited on a metal substrate. The metal substrate chosen for this study is stainless steel type SS-316L with very low carbon content. Surface modification on SS-316L will be carried out using TCP biomaterial through the electrophoretic deposition technique at room temperature.

EXPERIMENTAL PROCEDURES

Materials And Preparation

A commercial SS-316L with dimensions of 20 mm × 10 mm × 3 mm was used as the substrate. Before the coating process, the substrate surface was mechanically ground using silicon carbide (SiC) abrasive paper ranging from P120 to P1200 grit to achieve a uniform surface roughness. The samples were then cleaned using methanol and distilled water and air-dried. Subsequently, the substrate was immersed in a 4% NaOH solution for 10 minutes, followed by pickling in a 1% HCl acid solution for an additional 10 minutes. Afterward, the substrate was cleaned with distilled water and methanol and air-dried.

Electrophoretic Deposition

EPD was carried out using a DC power supply. Two electrodes were prepared, with each SS316L acting as the cathode, and a graphite electrode was used as the anode in the EPD process, with a distance of 3 cm between the electrodes. The EPD process was conducted with a voltage of 10 for deposition times of 10, 20, and 30 minutes. The selection of this voltage is due to the better quality of the coating achieved at relatively low voltages to prevent layer peeling from the substrate (Assadian et al., 2015; Besra & Liu, 2007). The electrophoretic deposition scheme is illustrated in Figure 1.

The electrolyte solution was prepared by dissolving 0.064 M TCP or tricalcium phospahate [$Ca_3(PO_4)_2$] in distilled water. TCP (Shuren Food Additive, ISO9001/ISO22000) is a food product sold in the food industry as a food grade anti-caking agent. Nitric acid (HNO_3) was added to the electrolyte solution to lower the pH to 4.7. The electrolyte solution was continuously stirred at a speed of 100 rpm. The deposition process was carried out at room temperature. After the EPD process was completed, the substrate was air-dried at room temperature for 24 hours. The electrodeposition of TCP was carried out with different deposition time, which was 10 minutes for TCP10, 20 minutes for TCP20 and 30 minutes for TCP30.

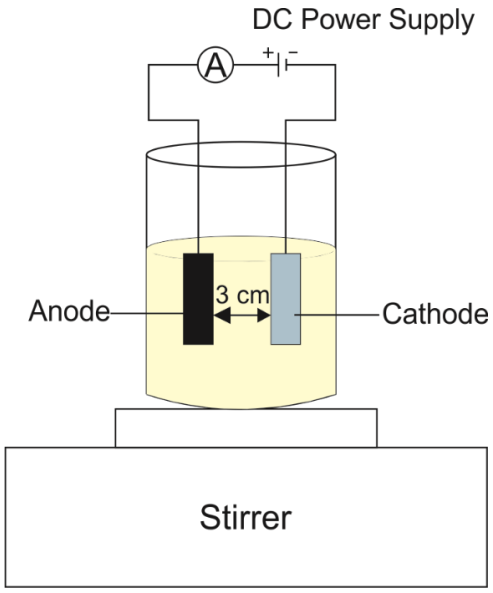

Figure 1. Scheme of TCP coating on SS316L using electrophoretic deposition.

Characterization

Chemical composition of the substrate was tested using optical emission spectroscopy (OES, ARL 3460, Switzerland). The morphology of the raw material and coated results was characterized using a scanning electron microscope (SEM; Rigaku, SU 3500; Japan). Chemical element observations from the coating results were conducted using energy-dispersive spectrometry (EDS; Rigaku, SU 3500; Japan). Hardness testing was performed using Vickers microhardness (Future Tech, Japan) with indentations of 50, 100, and 300 gf for 30 seconds. The results of the Vickers microhardness testing were calculated using the Eq. (1).

$$VHN = \frac{1.8544 \times P}{d_1 \times d_2} \quad (1)$$

where P is the indentation load, d_1 and d_2 are the diagonal distances of the indentation. Vickers microhardness testing is conducted to determine the hardness of both the substrate and its coating, with a specific focus on finding the optimal coating thickness value (Chicot et al., 1996). The calculation of the indentation depth is theoretically performed using Eq. (2).

$$h = \frac{d}{7} \quad (2)$$

where h is the indentation depth and d is the average diagonal of the indentation result (Iost et al., 2012).

RESULTS AND DISCUSSIONS

Deposition Yield

In this study, each process parameter is analyzed to determine the optimal results. One of the indicators in the parameter analysis is the calculation of the deposition yield (Ahmed & Rehman, 2020). The deposition yield can be calculated through Eq. (3).

$$Deposition\ yield = \frac{\Delta Weight\ (mg)}{A(mm^2)} \quad (3)$$

where ΔWeight is the difference in substrate weight between the initial condition and after EPD, and A is the coated surface. Table 1 shows the calculation results of the deposition yield and the hardness values of the substrate and TCP coatings. From Table 1, it can be concluded that a voltage of 10 V with a coating time of 30 minutes has the highest deposition yield. This deposition yield value indicates that the larger the value, the better the results of the deposition performed.

Table 1. Experimentally calculated deposition yield for SS316L/TCP coatings.

Sample	Deposition time (min)	ΔWeight (mg)	Deposition yield (mg/mm^2)
TCP10	10	40	0.119
TCP20	20	180	0.450
TCP30	30	270	0.635

Table 2. Chemical composition of the SS316L.

Steel	C	Si	Mn	Ni	Cr	Mo	V	Fe
wt.%	0.03	0.52	1.44	9.45	16.24	2.08	0.09	Bal.

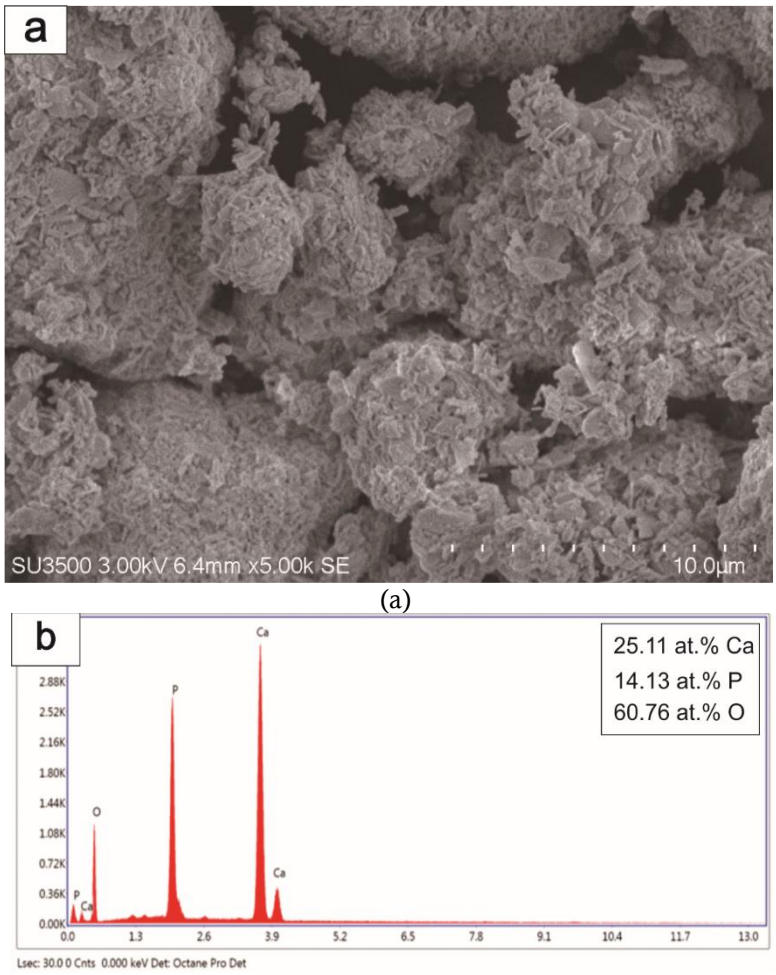

Figure 2. (a) Morphology and (b) chemical composition of TCP-$Ca_3(PO_4)_2$.

Morphology and Chemical Composition of Raw Materials

Table 2 shows the results of OES testing on the substrate and standard material for SS316L. The OES test results indicate that the substrate is SS316L stainless steel material with a composition of 16.24 wt.% Cr, 9.45 wt.% Ni, and 2.08 wt.% Mo, and a very low carbon (C) content of 0.03 wt.% C. These composition values are in accordance with the standard composition of SS316L.

Figure 2 shows the results of the initial characterization using SEM-EDS of the raw material TCP used in this research. Based on the results of the secondary electron image (SEI) from SEM shown in Figure 2a, the powder of the TCP raw material has an irregular shape with various sizes. The TCP particles have varying sizes ranging from 10-30 µm. On the other hand, the EDS test results are shown in Figure 2b. The results indicate that the raw material used consists of a composition of 25.11 at. % Ca, 14.13 at.% P, and 60.67 at.% O.

SEM-EDS Analysis of Biomimetic Coating

The SEM-EDS test results for SS316L material coated with TCP at different deposition times are shown in Figure 3. As seen in Figure 3(a), the coating deposited over a period of 10 minutes appears denser and more uniform, exhibiting a plate-like morphology of TCP on the substrate surface. However, a relatively short coating time

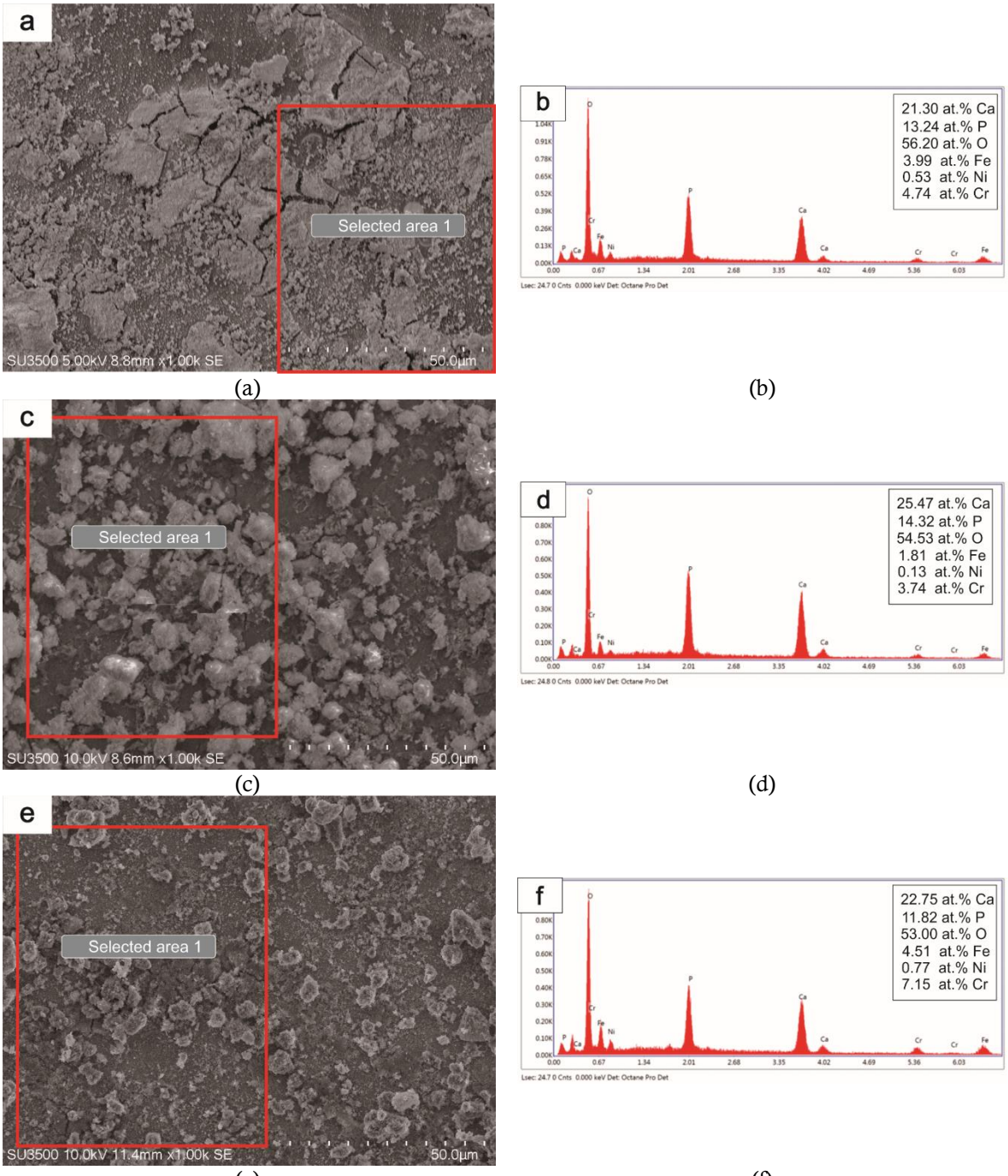

Figure 3. (a) SEM/EDS spectrum of TCP10, (b) EDS results of TCP 10, (c) SEM/EDS spectrum of TCP20, (d) EDS results of TCP 20, (e) SEM/EDS spectrum of TCP30, and (f) EDS results of TCP 30.

(10 minutes) shows signs of peeling and cracks on the substrate (Figure 3(a)). On the other hand, Figure 3(c) and d indicate that the coating results are not uniformly distributed, evidenced by the accumulation of TCP particles in certain areas. However, as the coating time increases, the TCP particles adhering to the substrate show reduced signs of peeling and cracking. The TCP layers deposited for 20 and 30 minutes exhibit irregular morphologies. Figure 4(a) also shows the analysis results in areas where TCP particles do not accumulate. Analysis performed using point scanning EDS techniques indicates the formation of a thin film layer in the specified area (Figure 4(b)).

These findings indicate that a longer deposition time enhances the adhesion capability of the TCP layer to the substrate, thereby reducing the occurrence of peeling in the coating layer.

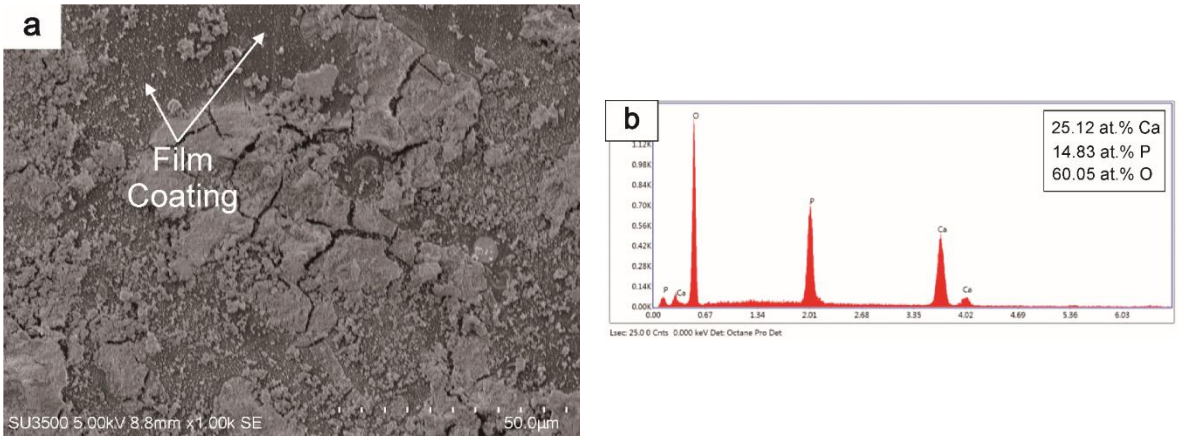

(a) (b)

Figure 4. (a) Morphology of SS316L-TCP10 at 1000x magnification and (b) chemical composition of the coating film on SS316L-TCP10.

Moreover, an increase in deposition time results in a change in the morphology of the coating layer. Additionally, the TCP layer formed on the SS316L substrate becomes thicker as the deposition time increases, as indicated by the weight gain after the deposition process in Table 2. The composition of the TCP layer is also identified in this study using EDS, as shown in Figures 3(b), (d), and (f). The EDS results reveal that there is no significant change in the composition of the TCP layer over different deposition time ranges.

Figure 5 shows a cross-sectional view between SS316L and the TCP layer with a deposition time of 30 minutes. The cross-sectional cut indicates two different morphologies formed from the deposition results. The TCP layer formed on the substrate surface has a dense structure and forms micro-sized plates. The deposited TCP layer on SS316L has a thickness ranging from 48.7 to 57.9 µm.

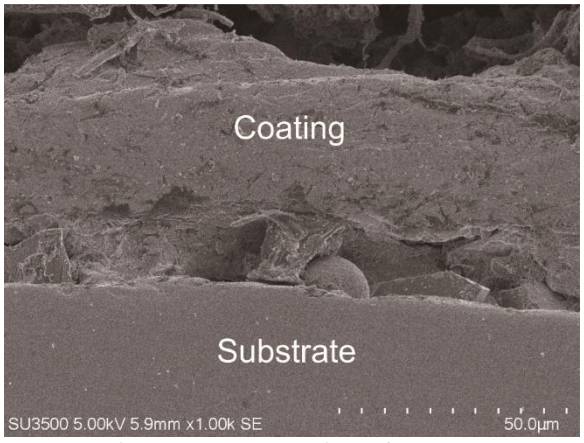

Figure 5. Cross-section of TCP30.

Hardness

Figure 6 presents a comparison of microhardness test results with indentation loads of 50 gf, 100 gf, and 300 gf for deposition times of 10, 20, and 30 minutes on the SS316L substrate. The hardness values of the SS316L substrate are influenced by the TCP layer. The highest hardness value is shown at the 50 gf load. This hardness value tends to decrease with increasing indentation load and coating thickness. The hardness test results are shown in Table 3. The decrease in hardness values is influenced by the presence of the TCP layer, which affects stress distribution during the indentation process. Therefore, in the TCP10 sample where the formed layer is thinner than TCP20 and TCP30, the hardness value approaches the hardness value of the substrate.

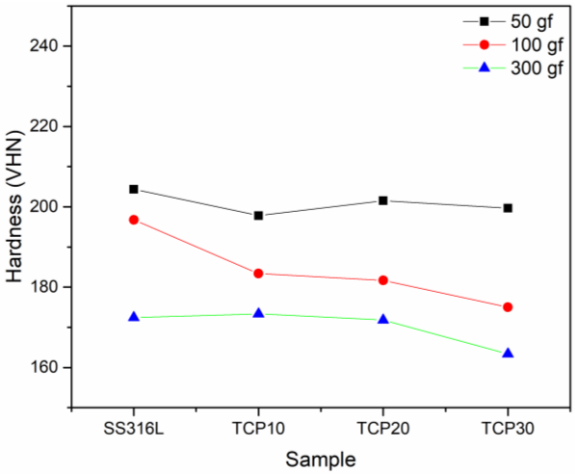

Figure 6. Vickers hardness result of SS316L/TCP coatings at 50, 100, and 300 gf.

Table 3. Hardness values for SS316L/TCP coatings.

Sample	Deposition time (min)	Hardness (VHN)		
		50 gf	100 gf	300 gf
SS 316L	-	204.37	196.76	172.44
TCP10	10	197.81	183.38	173.35
TCP20	20	201.52	181.66	171.83
TCP30	30	199.65	175.03	163.40

Hardness testing on human bones with indentation loads between 10-100 gf has also been conducted by several previous studies. The hardness test results on human bones fall within the range of 33-45 VHN (Coats et al., 2003; Dall'Ara et al., 2007). Therefore, it can be assumed that the lowest hardness value of the coating is desirable for use in the human body. This is because if the hardness of the implant material is very high, it can lead to the bones being more easily worn away when in contact with the implant material (Louvier-Hernández et al., 2021).

The values obtained from Vickers hardness testing are influenced by the diagonal lengths and the depth of the indentation produced. This is also affected by the indentation load applied. Micro-Vickers test results indicate that the increase in the thickness of the layer formed on the surface of SS316L and the increase in the applied indentation load will lead to a decrease in hardness values. This is because, with smaller loads, the influence of elastic deformation on the material becomes a significant factor in reducing the values of both diagonal lengths and indentation depth, resulting in higher hardness values. As the applied indentation load increases, the influence of elastic deformation on the material can be minimized, leading to lower hardness values compared to lower indentation loads.

The indentations from hardness testing also exhibit impressions in the form of circular depressions due to the distribution of stress between the substrate and coating surfaces. Figure 7 shows the detachment halo's diameter results against penetration depth and the indentation loading zone. The results indicate a linear relationship between the impression diameter, indentation depth (h), and indentation load. This suggests that higher loads will cause plastic deformation, resulting in larger impression diameters and apparent indentation depths.

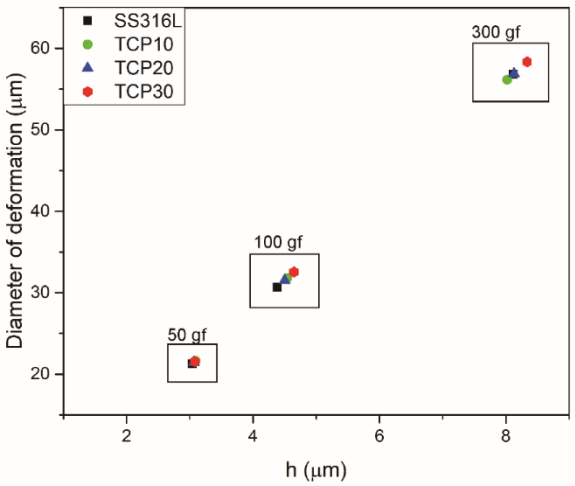

Figure 7. Diameter of the deformation against the depth penetration of the SS316L/TCP coatings.

CONCLUSION

In this study, the topic revolves around the deposition of TCP [$Ca_3(PO_4)_2$] on SS316L substrate with varying deposition times using the electrophoretic deposition technique. Samples were characterized to understand the changes in microstructure and mechanical properties resulting from the coating. The key findings from this study are (1) The highest deposition yield, with a value of 0.635, was observed in the deposition process with a time range of 30 minutes. (2) Microstructure testing results indicate that the TCP 10 sample has a more uniform $Ca_3(PO_4)_2$ layer, but there is peeling and cracking in the coating. TCP20 and TCP30 exhibit irregular morphology in some areas, with no observable peeling of the layer. Additionally, the deposition process yields coatings with thickness in the range of 48.7-57.9 µm. Hardness testing results show that an increase in deposition time and sample weight leads to a decrease in microhardness Vickers. The hardness test values also correlate with the applied indentation load, indicating that higher loads result in decreased hardness and increased indentation depth.

ACKNOWLEDGMENTS

The authors acknowledge financial support from the Bandung Polytechnic for Manufacturing.

REFERENCES

Ahmed, Y., Rehman, M. A. U. 2020. Improvement in the surface properties of stainless steel

via zein/hydroxyapatite composite coatings for biomedical applications. Surfaces and Interfaces. 20: 100589.

AlMangour, B., Luqman, M., Grzesiak, D., Al-Harbi, H., Ijaz, F. 2020. Effect of processing parameters on the microstructure and mechanical properties of Co–Cr–Mo alloy fabricated by selective laser melting. Materials Science and Engineering: A. 792: 139456.

Ananth, K. P., Nathanael, A. J., Jose, S. P., Oh, T. H., Mangalaraj, D., Ballamurugan, A. 2015. Controlled electrophoretic deposition of HAp/β-TCP composite coatings on piranha treated 316L SS for enhanced mechanical and biological properties. Applied Surface Science. 353: 189-199.

Anselme, K. 2000. Osteoblast adhesion on biomaterials. Biomaterials. 21(7): 667-681.

Assadian, M., Rezazadeh Shirdar, M., Idris, M. H., Izman, S., Almasi, D., Taheri, M. M., Abdul Kadir, M. R. 2015. Optimisation of electrophoretic deposition parameters in coating of metallic substrate by hydroxyapatite using response surface methodology. Arabian Journal for Science and Engineering. 40: 923-933.

Bai, Y., Neupane, M. P., Park, I. S., Lee, M. H., Bae, T. S., Watari, F., Uo, M. 2010. Electrophoretic deposition of carbon nanotubes–hydroxyapatite nanocomposites on titanium substrate. Materials Science and Engineering: C. 30(7): 1043-1049.

Bartmanski, M., Cieslik, B., Glodowska, J., Kalka, P., Pawlowski, L., Pieper, M., Zielinski, A. 2017. Electrophoretic deposition (EPD) of nanohydroxyapatite-nanosilver coatings on Ti13Zr13Nb alloy. Ceramics International. 43(15): 11820-11829.

Besra, L., Liu, M. 2007. A review on fundamentals and applications of electrophoretic deposition (EPD). Progress in materials science. 52(1): 1-61.

Boccaccini, A., Keim, S., Ma, R., Li, Y., Zhitomirsky, I. 2010. Electrophoretic deposition of biomaterials. Journal of the Royal Society Interface. 7(suppl_5): S581-S613.

Caicedo, J., Caicedo, H., Ramirez-Malule, H. 2020. Structural and chemical study of β–Tricalcium phosphate-chitosan coatings. Materials Chemistry and Physics. 240: 122251.

Chambard, M., Marsan, O., Charvillat, C., Grossin, D., Fort, P., Rey, C., Bertrand, G. 2019. Effect of the deposition route on the microstructure of plasma-sprayed hydroxyapatite coatings. Surface and Coatings Technology. 371: 68-77.

Chicot, D., Hage, I., Demarecaux, P., Lesage, J. 1996. Elastic properties determination from indentation tests. Surface and Coatings Technology. 81(2-3): 269-274.

Coats, A. M., Zioupos, P., Aspden, R. M. 2003. Material properties of subchondral bone from patients with osteoporosis or osteoarthritis by microindentation testing and electron probe microanalysis. Calcified Tissue International. 73: 66-71.

Dall'Ara, E., Öhman, C., Baleani, M., Viceconti, M. 2007. The effect of tissue condition and applied load on Vickers hardness of human trabecular bone. Journal of biomechanics. 40(14): 3267-3270.

Dorozhkin, S. V. 2015. Calcium orthophosphate deposits: Preparation, properties and biomedical applications. Materials Science and Engineering: C. 55: 272-326.

Drevet, R., Benhayoune, H. 2022. Electrodeposition of Calcium Phosphate Coatings on Metallic Substrates for Bone Implant Applications: A Review. Coatings. 12(4): 539.

Drevet, R., Zhukova, Y., Malikova, P., Dubinskiy, S., Korotitskiy, A., Pustov, Y., Prokoshkin, S. 2018. Martensitic transformations and mechanical and corrosion properties of Fe-Mn-Si alloys for biodegradable medical implants. Metallurgical and materials transactions A. 49: 1006-1013.

Farrakhov, R., Melnichuk, O., Parfenov, E., Mukaeva, V., Raab, A., Sheremetyev, V., Prokoshkin, S. 2021Comparison of biocompatible coatings produced by plasma electrolytic oxidation on cp-Ti and Ti-Zr-Nb superelastic alloy. Coatings. 11(4): 401.

Fiume, E., Magnaterra, G., Rahdar, A., Verné, E., Baino, F. 2021Hydroxyapatite for biomedical applications: A short overview. Ceramics. 4(4): 542-563.

Gao, A., Hang, R., Bai, L., Tang, B., Chu, P. K. 2018. Electrochemical surface engineering of titanium-based alloys for biomedical application. Electrochimica Acta. 271: 699-718.

Ghasemi-Mobarakeh, L., Kolahreez, D., Ramakrishna, S., Williams, D. 2019. Key terminology in biomaterials and biocompatibility. Current Opinion in Biomedical Engineering. 10: 45-50.

Gheno, R., Cepparo, J. M., Rosca, C. E., Cotten, A. 2012. Musculoskeletal disorders in the elderly. Journal of clinical imaging science. 2: 39.

Heimann, R. B. 2016. Plasma-sprayed hydroxylapatite-based coatings: chemical, mechanical, microstructural, and biomedical properties. Journal of thermal spray technology. 25(5): 827-850.

Hosseinalipour, S., Ershad-Langroudi, A., Hayati, A. N., Nabizade-Haghighi, A. 2010. Characterization of sol–gel coated 316L stainless steel for biomedical applications. Progress in Organic Coatings. 67(4): 371-374.

Iost, A., Guillemot, G., Rudermann, Y., Bigerelle, M. 2012. A comparison of models for predicting the true hardness of thin films. Thin Solid Films. 524: 229-237.

Kollath, V. O., Chen, Q., Closset, R., Luyten, J., Traina, K., Mullens, S., Cloots, R. 2013. AC vs. DC electrophoretic deposition of hydroxyapatite on titanium. Journal of the European Ceramic Society. 33(13-14): 2715-2721.

Koumya, Y., Ait Salam, Y., Khadiri, M. E., Benzakour, J., Romane, A., Abouelfida, A., Benyaich, A. 2021Pitting corrosion behavior of SS-316L in simulated body fluid and electrochemically assisted deposition of hydroxyapatite coating. Chemical Papers. 75: 2667-2682.

Kurgan, N. 2013. Effects of sintering atmosphere on microstructure and mechanical property of sintered powder metallurgy 316L stainless steel. Materials & Design (1980-2015). 52: 995-998.

Li, G., Thabane, L., Papaioannou, A., Ioannidis, G., Levine, M. A., Adachi, J. D. 2017. An overview of osteoporosis and frailty in the elderly. BMC musculoskeletal disorders. 18: 1-5.

Louvier-Hernández, J., García, E., Mendoza-Leal, G., Flores-Flores, T., Flores-Martínez, M., Rodríguez de Anda, E., Hernández-Navarro, C. 2021. Effect of the variation of the electrodeposition time of hydroxyapatite/chitosan coatings on AISI 316L SS. Journal of Composite Materials. 55(29): 4421-4430.

Ma, Y., Talha, M., Wang, Q., Zhou, N., Li, Z., Lin, Y. 2022. A multifunctional coating with modified calcium phosphate/chitosan for biodegradable magnesium alloys of implants. New Journal of Chemistry. 46(9): 4436-4448.

Nkonta, D. T., Drevet, R., Fauré, J., Benhayoune, H. 2021. Effect of surface mechanical attrition treatment on the microstructure of cobalt–chromium–molybdenum biomedical alloy. Microscopy Research and Technique. 84(2): 238-245.

Olivier, F., Picard, Q., Delpeux-Ouldriane, S., Chancolon, J., Warmont, F., Sarou-Kanian, V., Bonnamy, S. 2020a. Influence of electrochemical parameters on the characteristics of sono-electrodeposited calcium phosphate-coated carbon fiber cloth. Surface and Coatings Technology. 389: 125507.

Olivier, F., Rochet, N., Delpeux-Ouldriane, S., Chancolon, J., Sarou-Kanian, V., Fayon, F., Bonnamy, S. 2020b. Strontium incorporation into biomimetic carbonated calcium-deficient hydroxyapatite coated carbon cloth: Biocompatibility with human primary osteoblasts. Materials Science and Engineering: C. 116: 111192.

Popescu-Pelin, G., Sima, F., Sima, L., Mihailescu, C., Luculescu, C., Iordache, I., Mihailescu, I. 2017. Hydroxyapatite thin films grown by pulsed laser deposition and matrix assisted pulsed laser evaporation: Comparative study. Applied Surface Science. 418: 580-588.

Safavi, M. S., Surmeneva, M. A., Surmenev, R. A., Khalil-Allafi, J. 2021RF-magnetron sputter deposited hydroxyapatite-based composite & multilayer coatings: A systematic review from mechanical, corrosion, and biological points of view. Ceramics International. 47(3): 3031-3053.

Shao, Z., Xia, J., Zhang, Y., Jiang, H., Li, G. 2016. Preparation of calcium

phosphate/chitosan membranes by electrochemical deposition technique. Materials and Manufacturing Processes. 31(1): 53-61.

Sheremetyev, V., Dubinskiy, S., Kudryashova, A., Prokoshkin, S., Brailovski, V. 2022In situ XRD study of stress-and cooling-induced martensitic transformations in ultrafine-and nano-grained superelastic Ti-18Zr-14Nb alloy. Journal of Alloys and Compounds. 902: 163704.

Shirkhanzadeh, M. 1998. Direct formation of nanophase hydroxyapatite on cathodically polarized electrodes. Journal of Materials Science: Materials in Medicine. 9: 67-72.

Surmenev, R. A., Ivanova, A. A., Epple, M., Pichugin, V. F., Surmeneva, M. A. 2021. Physical principles of radio-frequency magnetron sputter deposition of calcium-phosphate-based coating with tailored properties. Surface and Coatings Technology. 413: 127098.

Surmeneva, M. A., Ivanova, A. A., Tian, Q., Pittman, R., Jiang, W., Lin, J., Surmenev, R. A. 2019. Bone marrow derived mesenchymal stem cell response to the RF magnetron sputter deposited hydroxyapatite coating on AZ91 magnesium alloy. Materials Chemistry and Physics. 221: 89-98.

Trincă, L. C., Burtan, L., Mareci, D., Fernández-Pérez, B. M., Stoleriu, I., Stanciu, T., Souto, R. M. 2021. Evaluation of in vitro corrosion resistance and in vivo osseointegration properties of a FeMnSiCa alloy as potential degradable implant biomaterial. Materials Science and Engineering: C. 118: 111436.

Tulinski, M., Jurczyk, M. 2012Nanostructured nickel-free austenitic stainless steel composites with different content of hydroxyapatite. Applied Surface Science. 260: 80-83.

Vidal, E., Buxadera-Palomero, J., Pierre, C., Manero, J. M., Ginebra, M.-P., Cazalbou, S., Rodríguez, D. 2019Single-step pulsed electrodeposition of calcium phosphate coatings on titanium for drug delivery. Surface and Coatings Technology. 358: 266-275.

Yuan, J., Dai, B., Cui, X., Li, P. 2023. The effects of electrodeposition temperature on morphology and corrosion resistance of calcium phosphorus coatings on magnesium alloy: comparative experimental and molecular dynamics simulation studies. RSC advances. 13(48): 34145-34156.